JOURNAL OF THERMOPHYSICS AND HEAT TRANSFER
Vol. 21, No. 1, January–March 2007

Novel Method for Measurement of Total Hemispherical Emissivity

Saeed Moghaddam,* John Lawler,† and Joseph Currano‡
Advanced Thermal and Environmental Concepts (ATEC, Inc.), College Park, Maryland 20740
and
Jungho Kim§
University of Maryland, College Park, Maryland, 20742

DOI: 10.2514/1.26181

A heat flux-based method for measuring the emissivity of a surface is described. The emissivity is calculated by directly measuring the heat flux passing through the surface using a heat flux gauge. Unlike storage-based calorimetric methods, this method does not require application of known amounts of heat to the surface or the temperature history of a known amount of thermal mass to calculate the surface emissivity. Application and operation of this method is much simpler than calorimetric methods because it does not require careful thermal insulation of the substrate from the surroundings. This technique allows emissivity measurements of the newly developed variable emissivity surfaces with significantly lighter and more energy-efficient measurement equipment that can operate for long term space missions and allows emissivity measurement of more than one surface simultaneously on the same test substrate. In this study, a commercially available thermopile heat flux sensor was used to measure the emissivity of a black paint and a variable emissivity surface, called electrostatic switched radiator. This paper details the concept, experimental setup, and the experiment results.

Nomenclature

A	=	area
F	=	view factor
q	=	heat flux, W
T	=	temperature, K
ϵ	=	emissivity
σ	=	Stefan–Boltzmann constant

Subscripts

1, 2	=	generic surfaces
1–2	=	from surface 1 to surface 2
S	=	surface
∞	=	far field

Introduction

RECENT developments in variable emissivity surfaces and the need for their testing in space environments have generated a demand for emissivity measurement equipment that is lighter, more efficient, and less complex than conventional emissivity measurement techniques. Unlike traditional constant emissivity surfaces such as paints and films, the new variable emissivity surfaces are more complex in structure and performance. Variable emissivity surfaces can be based on different concepts such as changing the optical properties of the surface material itself or modifying the surface structurally to alter its radiation heat transfer performance. Polymer-based materials [1] and inorganic thin films [2,3] can have surfaces with variable optical properties. Two structurally active surfaces under development are electrostatic devices [4,5], also called electrostatic switched radiator (ESR), and microelectromechanical systems (MEMS) louvers [6]. An ESR operates in vacuum by opening and closing a gap between two surface layers via electrostatic forces, with the gap hindering heat transfer through the surface layers. The effective emissivity is controlled by making the base layer a low emissivity surface and the top layer a high emissivity surface. With voltage applied, the top layer is attracted to the base layer allowing heat to conduct into the top layer, and so the effective emissivity is approximately that of the top layer. In the deactivated state, the gap between the layers prevents conduction. Heat must radiate from the base layer to the top layer before radiating outward, so that the effective emissivity is closer to that of the base layer [4,5]. The MEMS louvers are microfabricated versions of the larger scale louvers that were developed earlier for spacecraft, in which vanes are opened and closed to vary the effective emissivity of a surface [6]. The acceptance of these active thermal control systems requires a demonstration of their performance in a relevant space environment.

The most common methods used for measuring the emissivity of a surface are calorimetric and optical methods. Calorimetry involves measuring the heat power delivered to the test sample as well as the temperatures of the emitting surface (the sample) and the surroundings in a vacuum over time [7,8]. An energy balance is then used to determine the emissivity. The sample must be well insulated on the sides and back, and parasitic heat losses must be accounted for to accurately determine the heat transfer through the sample surface. Optical techniques involve illuminating a sample with infrared energy and measuring the percentage of energy reflected from the surface [9]. The absorptance is calculated from the reflectance and used to calculate normal emittance by Kirchhoff's law and the Stefan–Boltzmann equation. The optical method is generally less labor intensive than the calorimetric method, but the measurements must be repeated at all angles and then numerically integrated to accurately obtain the total hemispherical emissivity. In many cases this is not practiced and the normal emissivity is considered as an approximation of the hemispherical emissivity. Although the complexity of measuring the emissivity of spatially and temporally variable emissivity surfaces can be overcome using sophisticated testing equipment designed for conventional emissivity measurement techniques in a lab environment, the

Received 26 June 2006; revision received 26 August 2006; accepted for publication 27 August 2006.

*Vice President of Research and Development, 7100 Baltimore Avenue, Suite 300.
†President, ATEC, 7100 Baltimore Avenue, Suite 300.
‡Research Assistant, ATEC, 7100 Baltimore Avenue, Suite 300, and Graduate Student, University of Maryland.
§Associate Professor, Department of Mechanical Engineering, 2181 Martin Hall, University of Maryland.

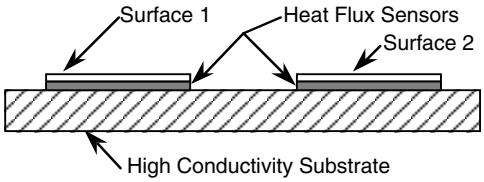

Fig. 1 Schematic showing the arrangement of heat flux sensors with respect to the emitting surface.

application of such systems in space is associated with a significant weight, energy consumption, and data volume.

The advantage of the heat flux-based (HFB) method is that it measures the hemispherical emissivity without the need for careful thermal insulation of the substrate or multiple optical measurements at different angles. The HFB method can measure spatial variations of emissivity without the complexity and labor intensity of the optical method. Furthermore, the HFB method provides real-time measurement of the surface emissivity through direct measurement of heat flow through the emitting surface. The HFB method requires minimal data measurement and processing. The heat flux passed through the surface (measured directly by a heat flux sensor), the surface temperature, and the enclosure temperature are the only information required to calculate the surface emissivity, as long as radiation is the only significant mode of heat transfer from the surface to the enclosure. This method requires neither the temperature history nor thermal insulation of the substrate on which the variable emissivity surface is installed. In addition to its simplicity and significantly reduced data volume, the HFB emissivity measurement method eliminates the need for heaters and their power measurement equipment, control system, and more important, heating energy that is at a premium in any space mission. The HFB method can measure the emissivity of an active surface such as an ESR while it is operating as part of a space vehicle's thermal control system.

In the HFB method, the heat flux through the emitting surface is directly measured using one or more (depending on the required spatial resolution) heat flux sensors placed between the active (or passive) sample surface and the substrate on which the surface is installed. The low thermal capacitance of the available heat flux sensors can provide good temporal resolution of the heat flux. The small size of the sensors can provide the necessary spatial resolution to resolve the performance of a spatially variable emissivity surface if desired. The HFB method also allows multiple surfaces with different emissivities to be tested simultaneously. The objective of this work is to demonstrate the capability of the HFB method in measuring the emissivity of passive and active surfaces. The passive surface used in this study is a black paint (Rustoleum Painter's Touch flat black) and the active surface is an ESR manufactured by Sensortex, Inc. A space experiment that incorporates the HFB emissivity measurement method is briefly discussed.

Heat Flux-Based Emissivity Measurement

In the HFB method, a heat flux sensor is installed between the surface whose emissivity is being measured and a high conductivity substrate. Figure 1 shows a schematic of this configuration. The heat emitted from the surface passes through the heat flux sensor. Knowing the heat flux through the sensor, the total hemispherical emissivity of the surface can be calculated using the Stefan–Boltzmann law of radiation:

$$\varepsilon = \frac{q''}{\sigma(T_S^4 - T_\infty^4)} \tag{1}$$

In this equation, q'' is the heat flux per unit area (W/m^2), which is the quantity measured by the heat flux sensor. The temperature of the surface T_S is approximated by the temperature of the substrate. It should be noted that the direct measurement of the heat flux through the gauge makes the parasitic heat loss/gain irrelevant to the measurement of emissivity, because any parasitic heat paths simply change the surface temperature, which is included in the calculation.

In this study, two different sizes of heat flux sensors were used. Both sensors (shown in Fig. 2) were fabricated by the RDF Corporation and consist of many thermocouple pairs deposited on either side of a thin polyimide film and arranged to form a thermopile. Heat passing through the gauge produces a temperature difference across the film resulting in an electromotive force (EMF) at the output leads. First, a standard heat flux sensor (RDF 27160) was used to demonstrate the capability of the HFB method in measuring the emissivity of a passive coating (black paint). Second, a larger heat flux sensor was custom made to accommodate the size of an ESR device. The size of the standard sensor was 11.9 mm × 46.2 mm, and the size of the custom made sensor was 50.8 mm × 50.8 mm. The average nominal sensitivity of the RDF 27160 was 0.92 $\mu V/(W/m^2)$ at 21°C, and the sensitivity of the large sensor was 6.499 $\mu V/(W/m^2)$. This value is temperature dependent; the temperature correction factors are available from the manufacturer. The sensors were calibrated by the manufacturer with an uncertainty of 3–5%.

Experimental Setup

Three RDF 27160 sensors were painted black and attached using an epoxy phenolic (Vishay Micro-Measurements M-Bond 600) to a 76.2 mm × 76.2 mm × 6.35 mm copper block (Fig. 3). Two Minco Products' flexible heaters were attached to the opposite side of the copper block, so its temperature could be controlled during the experiment. Because the substrate is small (76.2 mm × 76.2 mm× 6.35 mm) and made of copper, it was considered isothermal. The substrate temperature was measured by four thermocouples each placed on one edge of the substrate, and the average measurement was used as the surface temperature.

A vacuum chamber was designed and fabricated to conduct the experiment on the heat flux sensors and copper block assembly in a high vacuum environment, so that heat loss through convection and conduction to the air could be eliminated. The vacuum chamber consisted of a 25.4 cm diam cylindrical basin, 22.9 cm deep with 0.32 cm thick walls and bottom, capped with a 2.54 cm thick by 30.5 cm diam stainless steel flange. The lid had four feedthroughs

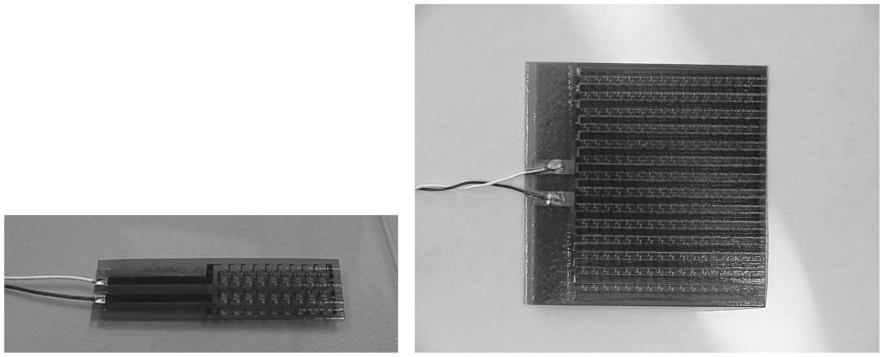

a) **b)**

Fig. 2 Photographs of two RDF heat flux sensors: a) Model 27160; b) large custom-made sensor.

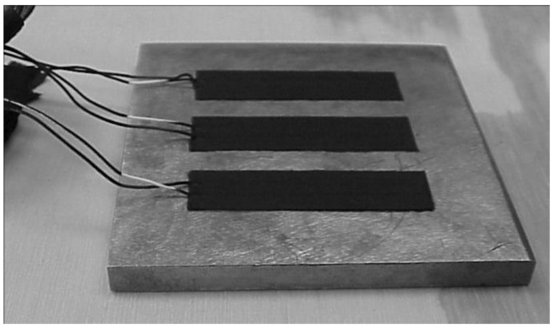

Fig. 3 Three heat flux sensors (painted black) attached to a copper plate.

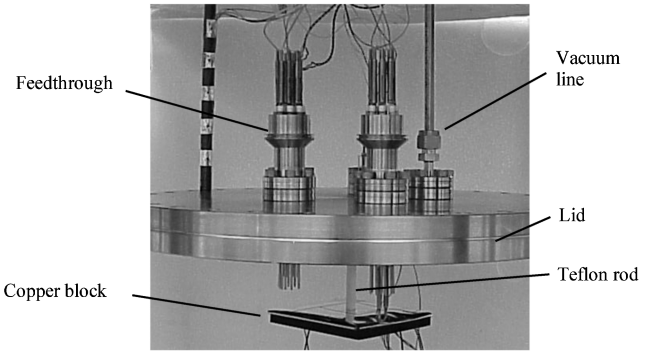

Fig. 4 Vacuum chamber lid, feedthroughs, and copper block assembly.

allowing for connection of thermocouples, heat flux sensors, power wires for the heaters, and wires for the excitation voltage of the active emissivity surface when it was tested. The basin wall temperature was measured using three thermocouples installed at different locations. The chamber was connected by a 1.27 cm outer diameter tube to the vacuum system, which consists of a turbomolecular pump and a roughing pump, together capable of sustaining a pressure of 10^{-8}–10^{-10} bar inside the chamber. A pressure of 10^{-8} bar is low enough (given the chamber's size) to reduce the effective thermal conductivity of air to 0.8% of its thermal conductivity at atmospheric pressure [10], thus eliminating conduction from the heated surface to the remaining gas. The pressure was measured between the turbopump and the vacuum chamber and was monitored to ensure that it was lower than 10^{-8} bar (7.5×10^{-6} torr) before beginning each radiation test. Four 0.95 cm threaded rods screwed into the top flange supported the chamber when suspended inside a liquid nitrogen Dewar flask. A 0.64 cm diam Teflon rod 5 cm long was used to suspend the copper block underneath the chamber lid. Figure 4 shows the assembly of the chamber lid, feedthroughs, and the copper block. Figure 5a shows the vacuum chamber fully assembled, and Fig. 5b shows the vacuum chamber installed inside the Dewar flask.

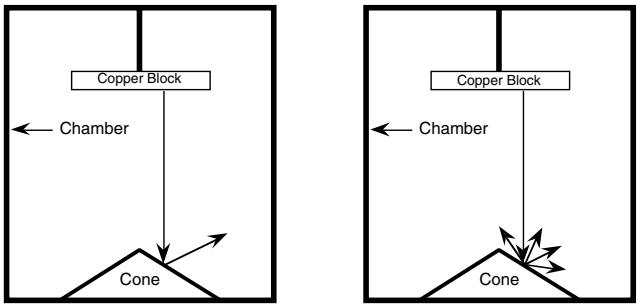

a) **b)**

Fig. 6 Schematic of the cone position inside the chamber a) as an idealized nondiffuse surface, and b) as a diffuse surface.

A data acquisition system was used to record temperature and heat flux sensor readings.

The inside of the vacuum chamber was painted black. To prevent the heated surface from seeing its reflection on the bottom of the chamber, a cone was fabricated and attached to the bottom of the chamber as shown in Fig. 6. This arrangement increases the likelihood that multiple reflections occur (Fig. 6a) before the emitted radiation returns to the copper block. However, because the cone and wall are in reality more like diffuse emitters, it is still possible that some reflection would reach the test surface, as shown in Fig. 6b. This is accounted for by the fact that the area of the sample surface is much smaller than the inside surface of the chamber, so that the test surface was essentially radiating to a blackbody at liquid nitrogen temperature (−195°C) when the Dewar was filled. The heat flux from the test surface to the enclosure can be written as a two node, source-sink radiation network [11]:

$$q_{1\text{–}2} = \frac{\sigma T_1^4 - \sigma T_2^4}{[(1-\varepsilon_1)/\varepsilon_1 A_1] + (1/A_1 F_{1\text{–}2}) + [(1-\varepsilon_2)/\varepsilon_2 A_2]} \tag{2}$$

where surface 1 is the test surface and surface 2 is the inner walls of the vacuum chamber (including the cone). Since $F_{1\text{–}2} = 1$ and if $A_2 \gg A_1$, the equation reduces to

$$q_{1\text{–}2} = \left(\sigma T_1^4 - \sigma T_2^4\right)\varepsilon_1 A_1 \tag{3}$$

which is the same as Eq. (1). In this experimental setup, $A_2 \approx 90A_1$ for the ESR on a large heat flux sensor, and $A_2 \approx 420A_1$ for the small heat flux sensor. An approximation of the numerical error due to this blackbody assumption is given in the Uncertainty Analysis section.

Experimental Procedure for Testing the Black Paint

The Dewar flask was gradually charged with liquid nitrogen. Less than 1 h was required for the entire vacuum chamber assembly to reach liquid nitrogen temperature (−195°C), as indicated by the six thermocouples installed at different locations on the internal surface

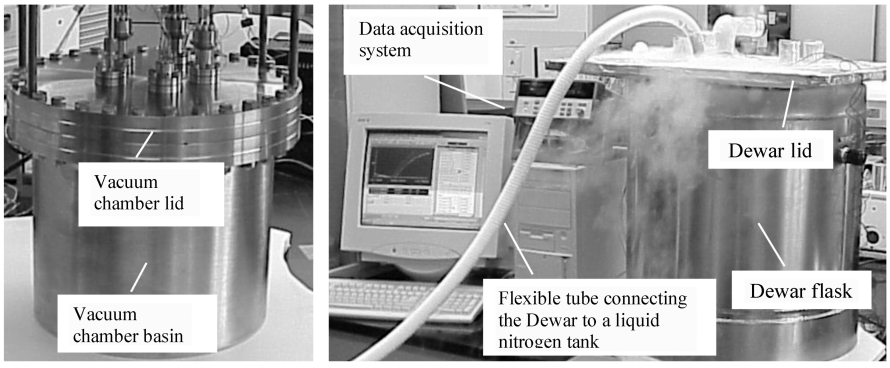

a) **b)**

Fig. 5 Photographs of a) vacuum chamber assembly and b) experimental setup.

of the vacuum chamber (basin and lid). In "sweep" tests, electrical power was supplied to the heaters until the substrate reached 60°C, after which the heaters were turned off. The substrate temperature and the output of the heat flux sensors were then recorded as the substrate cooled down to −50°C over a period of 2.5 h. In "step" tests, a series of discrete power levels were supplied to the heaters on the copper block, and the steady-state sensor readings and substrate temperatures were recorded at each power level. The pressure in both the sweep and step tests was about 9×10^{-9} bar (6.8×10^{-6} torr).

Test Results with Black Paint

The heat flux values were obtained by dividing the measured output voltages from the heat flux sensors by their sensitivities or calibration constants [$\mu V/(W/m^2)$]. The sensitivity for each sensor at a reference temperature as well as the correction factors to adjust these sensitivity values for temperature were supplied by the manufacturer.

The heat flux as a function of surface temperature is shown in Fig. 7 for one representative sensor. It includes data obtained from both the sweep and step tests. Also included is the heat flux that should be generated over this range of temperatures if the emissivity of the surface is 0.90. The heat fluxes measured via the sweep and step experiments are in excellent agreement with the calculated values.

The heat fluxes, the average block temperatures, and the average chamber temperatures were then used to calculate the emissivity obtained simultaneously from three sensors mounted on the copper block (Fig. 8). The emissivity values for the flat black paint are in the expected ranges of 0.85–0.95. The emissivity is essentially independent of temperature from about 60°C down to −50°C. The difference in reading of the three heat flux sensors is less than 5%, which is consistent with their calibration accuracy.

To compare the results with an independent measurement, a 5-mil thick polyimide film (the same material as the heat flux sensor) was painted with the same black paint used on the heat flux sensors and sent to Sheldahl Corporation for an optical measurement of its emissivity. Sheldahl uses a Lion Research Corporation emissometer to estimate total hemispherical emissivity according to "Method B," as described in ASTM Standard E408. The emissometer responds to broadband (3–30 μm) IR energy, and the measurement was only made at ambient temperature. Sheldahl measured the emissivity of the black paint surface as 0.90 (Fig. 8), which is in excellent agreement with the HFB data.

ESR Assembly and Testing

To demonstrate the capability of the HFB method in measurement of the rapid changes in emissivity of an ESR device, a test module incorporating a heat flux sensor and an ESR device was assembled by Sensortex, Inc. A schematic cross section of the test unit built on a

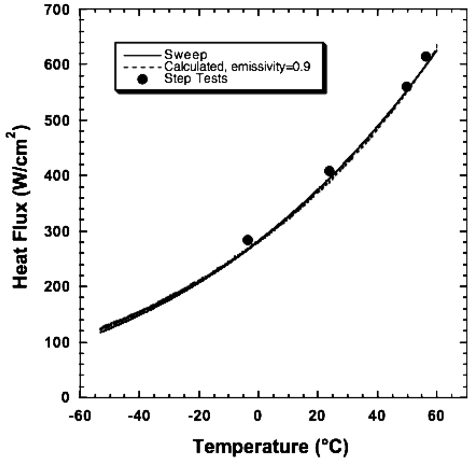

Fig. 7 Heat flux as a function of block temperature.

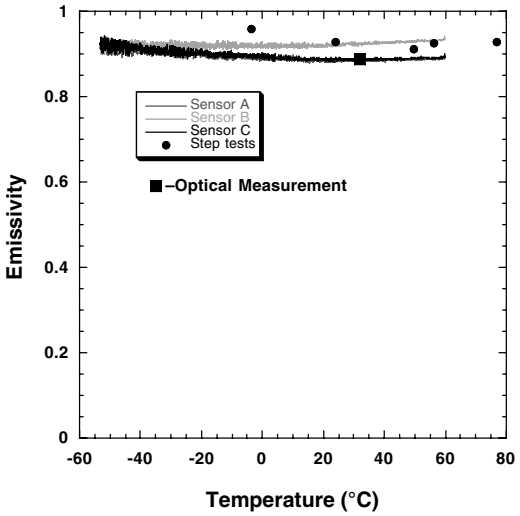

Fig. 8 Emissivities of sensors coated with black paint as functions of temperature.

76.2 mm × 76.2 mm × 6.35 mm aluminum substrate is shown in Fig. 9. A large heat flux sensor was attached to the substrate with a thermally conductive film epoxy (Emerson & Cuming CF3350), and a thin (0.813 mm) aluminum plate was epoxied to the top of the heat flux sensor. The aluminum plate has a tab at one corner so a high voltage lead can be attached and serves as the high voltage side when the ESR is actuated. A 12.7 μm thick film of Kapton was then epoxied to the aluminum plate to serve as an electrical insulator. Finally, the corners of the ESR membrane were attached on the Kapton layer, so that the membrane is suspended loosely over the Kapton insulating layer when the ESR is not actuated. In this configuration, when a ground lead is attached to the backside of the membrane (backside of the membrane is metallized and has a low emissivity) and a high voltage is applied to the lead attached to the aluminum plate, the ESR is actuated and clings tightly to the surface. This changes the heat transfer mode between the membrane and the surface beneath it from radiation to conduction. In this mode, the emissivity of the device is very close to the emissivity of the front side of the membrane (about 0.84).

A heater was attached to the backside of the aluminum substrate. The ESR substrate was suspended inside the vacuum chamber the same way as the copper substrate with the small heat flux sensors. The Dewar was filled with liquid nitrogen as before, so that the chamber reached −195°C. The pressure during testing was about 6.4×10^{-9} bar (4.8×10^{-6} torr). Heat was applied to the substrate so that it remained at a constant temperature, and the ESR was allowed to radiate energy to the chamber walls. Before each test, the temperature of the substrate was raised or lowered to a desired value and allowed to reach steady state. The tests were started with the ESR deactivated, and then 315 VDC was applied to actuate it. Heat flux passing through the device was continuously measured by the heat flux sensor.

Test Results on ESR

Results are shown in Fig. 10. When the ESR is not activated, a small gap exists between the membrane and the Kapton layer, inhibiting heat flux to the membrane and thus through the ESR. When the ESR is actuated, a sharp increase in heat flux occurs at the surface, which is a combination of the now higher radiation being emitted by the ESR, and a transient portion due to sensible heating of

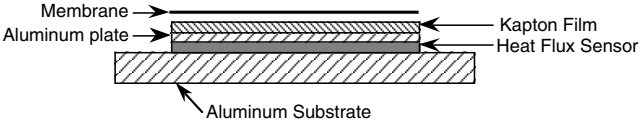

Fig. 9 Schematic of ESR on aluminum substrate (not to scale).

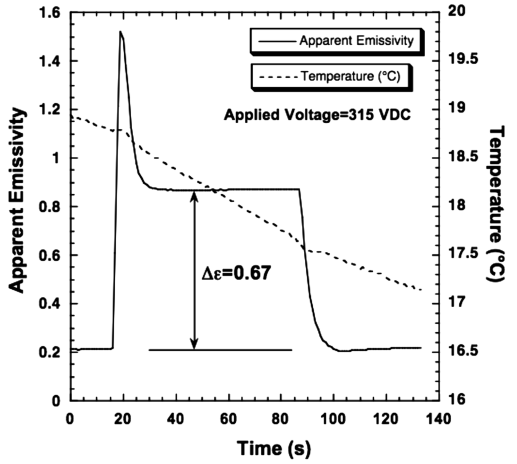

Fig. 10 Apparent emissivity and substrate temperature as functions of time during actuation (315 V) of ESR at 18°C.

the membrane by conduction. This transient portion of the heat flux dissipates in about 12 s, and the apparent emissivity of the surface stabilizes at a value 0.67 higher than the device's deactivated emissivity.

Uncertainty Analysis

An analysis of the experimental errors was conducted to determine the uncertainty in the emissivity measurements. First, an uncertainty was calculated assuming the vacuum chamber acts as a blackbody with no radiation reflected back to the test surface. A calculation of emissivity with diffuse radiation was then carried out using Eq. (2) instead of Eq. (1), with data from one test run with the small heat flux sensor and one run with the ESR. The chamber walls were painted with the same black spray paint that was tested on the small heat flux sensors, which were also measured optically by Sheldahl ($\epsilon = 0.9$). In general, black paint is considered to have an emissivity of 0.85 or higher. With the most conservative estimation of 0.85 for the black-painted chamber walls, the emissivity calculated from Eq. (2) differs by less than 0.2% (± 0.0014) from Eq. (1) for the activated ESR (0.3% when deactivated); and less than 0.05% (± 0.0004) for a small heat flux sensor. The error is even smaller if the emissivity of 0.9 measured by Sheldahl is used. This uncertainty is an order of magnitude smaller than the uncertainty due to measurement errors, so Eq. (1) was used for the remainder of the error analysis.

Another possible error investigated is the effect of radiation from the edges of the sensor and coatings. However, the geometry of the heat flux sensors is such that radiation from the edge of a sensor does not substantially affect the reading. The heat flux sensor is only 0.007 in. (0.1778 mm) thick, and the thermopile junctions closest to the edge are 0.025 in. (0.635 mm) from the edge. This distance is large enough that heat flowing through the sensing area will not radiate out the edge of the sensor and will only radiate out the edge of a test surface if it is very thick. In the case of the ESR, the thickness is dominated by the aluminum plate, which has a very low emissivity. Moreover, the area of the heat flux sensor edges is less than 4% of the top surface area even for a small heat flux sensor. Thus, radiation from the edges was considered negligible and not included in the uncertainty calculation. If the HFB method were used on a very thick surface, the heat flux measurement should be multiplied by the ratio of the total test surface area (including edges) to the top surface of the heat flux sensor.

The calculation of emissivity in Eq. (1) depends on the measurement of heat flux, surface temperature and the temperature of the vacuum chamber walls. Therefore, the thermocouple and heat flux sensor calibration errors as well as measurement errors in the data acquisition unit contribute to uncertainty in calculated emissivity. A root-mean-square analysis was used to combine these uncertainties as shown in Eq. (4):

$$\Delta\varepsilon = \sqrt{\left(\frac{\partial\varepsilon}{\partial q''}\Delta q''\right)^2 + \left(\frac{\partial\varepsilon}{\partial T_S}\Delta T_S\right)^2 + \left(\frac{\partial\varepsilon}{\partial T_\infty}\Delta T_\infty\right)^2} \quad (4)$$

The thermocouples used were type K with an uncertainty of ± 2.2°C for subzero and ± 1.1°C for above-zero temperatures. The heat flux sensors were calibrated by the manufacturer with a calibration accuracy of 3–5%. Because the heat flux sensor measurements also depend on a temperature correction factor, the error in the surface temperature measurement was combined with the heat flux sensor output error (calibration error and data acquisition error) to provide a root-mean-square error for the heat flux. The heat flux error $\Delta q''$ is given in terms of the output error ΔV and the surface temperature error ΔT_S as

$$\Delta q'' = \sqrt{\left(\frac{\partial q''}{\partial V}\Delta V\right)^2 + \left(\frac{\partial q''}{\partial T_S}\Delta T_S\right)^2} \quad (5)$$

This expression gave a maximum heat flux error of ± 32 W/m^2 (or 5.0%) for the black paint test on the small heat flux sensors at the highest temperature (i.e., highest heat flux) and ± 8.2 W/m^2 (6.6%) at the lowest temperature (and heat flux). For the ESR device, the maximum heat flux error was ± 19 W/m^2 in the steady activated state and ± 4.6 W/m^2 in the deactivated state.

As stated previously, the maximum heat flux uncertainty occurs at the highest temperature, which corresponds to the highest heat flux. However, inspection of the derivatives in Eq. (4) with the known temperature errors reveals that the maximum contribution from the temperature error occurs at the minimum (most negative) temperature. Because of this offsetting effect, the emissivity error was calculated at both extremes. For the test run with the small heat flux sensor coated with the black paint, the emissivity uncertainty was calculated to be 5.1% of the measurement at the high temperature (60°C) and 7.0% of the measurement at the low temperature (−53°C). This is equivalent to an uncertainty of ± 0.047 at the high temperature and ± 0.066 at the low temperature. In the ESR test (17–19°C), the uncertainty was ± 0.046 in the activated state (high effective emissivity) and ± 0.012 in the deactivated state (low effective emissivity).

The temperature drop from the substrate to the surface can be estimated using simple 1-D conduction. Assuming a thermal conductivity of 0.5 W/m · K for the epoxy phenolic (M-Bond 600) used with the small heat flux sensors, and using the conductivity of Kapton (0.12 W/m · K) for the heat flux sensor, the temperature drop across these two layers is 0.9°C at the high end heat flux (600 W/m^2). For the ESR, including all layers (epoxy layers, sensor, conductor, insulator, and membrane), the temperature drop is estimated to be 1.0°C with the most significant temperature drop in both cases across the heat flux sensor itself. This temperature drop contributes an additional bias error (the actual surface temperature is always lower than the substrate temperature while it is emitting heat) of about 1.5% of the measured emissivity for the small heat flux sensors, and 1.6% for the ESR.

Adding the temperature error to the other measurement errors, the overall root-mean-squared error for the emissivity measurements by the small heat flux sensors is 5.3% at high temperature and 7.2% at low temperature. For the ESR, the overall emissivity error is 5.7% while activated and 6.1% while deactivated.

MISSE Space Test Package

To enable testing of the HFB emissivity measurement system and an active thermal control surface (ESR) in space, a module containing six heat flux sensors, two ESR surfaces, and their associated electronics was designed, fabricated, and tested. This module will be incorporated into MISSE-6 (Materials International Space Station Experiment),[¶] which is scheduled to be installed by a space shuttle crew on the exterior of the International Space Station

[¶]Data available on-line at http://misse1.larc.nasa.gov/ [cited 25 September 2006].

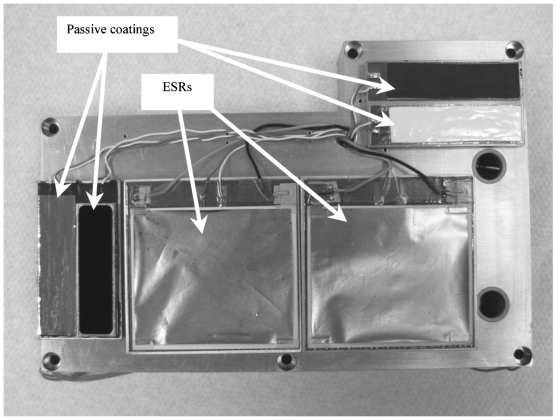

Fig. 11 Photograph of the MISSE module containing six HFB emissivity sensors. The two large sensors are for testing active thermal surfaces.

(ISS) in 2007. This testing is being conducted to demonstrate the ability of this technique to measure the emissivities of passive and active surfaces in a space environment over an extended period of time.

Electrical power for the MISSE-6 experiments is being supplied by the ISS during MISSE-6's deployment, but data telemetry is not included. Therefore, dataloggers will record readings from the six heat flux sensors, two photodiodes, and two thermocouples, and the actuation voltages of the ESRs every 19 min. Actuation voltages will be supplied to the ESRs for a period of 12 h every 24 h. The MISSE package will be retrieved about a year after deployment. A photograph of the module is shown in Fig. 11.

Conclusion

A new method has been developed for measuring the emissivity of surfaces over a wide range of temperatures. This method employs a more direct means for determining emissivity, making it ideal for studying multiple advanced variable emissivity coatings and structures simultaneously and for deploying on spacecraft. The use of heat flux sensors allows the measurement of the total hemispherical emissivity of surfaces with the temporal and spatial resolutions both to evaluate coatings that can change their emissivities and to monitor the changes in emissivities of surfaces exposed to space or other harsh environments.

Acknowledgments

The authors acknowledge and appreciate the support provided by their Air Force SBIR Phase I and II Contracts, FA8650-04-M-5020 and FA8650-05-C-5045, administered by the SBIR Program Office at the Air Force Research Laboratory, Wright–Patterson Air Force base. The Air Force technical monitor was Ming Chen. William Biter of Sensortex provided the ESR.

References

[1] Chandrasekhar, P., Zay, B. J., McQueeney, T., Ross, D. A., Lovas, A., Ponnappan, R., Gerhart, C., Swanson, T., Kauder, L., Douglas, D., Peters, W., and Birur, G., "Variable Emittance Materials Based on Conducting Polymers for Spacecraft Thermal Control," *Proceedings of the Space Technology and Applications International Forum (STAIF-2003)*, edited by M. El-Genk, AIP Conference Proceedings, No. 654, American Institute of Physics Press, Melville, NY, 2003, pp. 157–161.

[2] Kislov, N., Groger, H., and Ponnappan, R., "All-Solid-State Electrochromic Variable Emittance Coatings for Thermal Management in Space," *Proceedings of the Space Technology and Applications International Forum (STAIF-2003)*, edited by M. El-Genk, AIP Conference Proceedings No. 654, American Institute of Physics Press, Melville, NY, 2003, pp. 172–179.

[3] Hale, J. S., and Woollam, J. A., "Prospects for IR Emissivity Control Using Electrochromic Structures," *Thin Solid Films*, Elsevier, New York, 1999, Vol. 339, pp. 174–180.

[4] Biter, W., Oh, S., and Hess, S., "Electrostatic Switched Radiator for Space Based Thermal Control," *Proceedings of the Space Technology and Applications International Forum (STAIF-2002)*, edited by M. El-Genk, AIP Conference , No. 608, American Institute of Physics Press, Melville, NY, 2002, pp. 73–80.

[5] Biter, W., Hess, S., and Oh, S., "Electrostatic Appliqué for Spacecraft Temperature Control," *Proceedings of the Space Technology and Applications International Forum (STAIF-2003)*, edited by M. El-Genk, AIP Conference Proceedings, No. 654, American Institute of Physics Press, Melville, NY, 2003, pp. 162–171.

[6] Garrison, D. A., Osiander, R., Champion, J., Swanson, T., Douglas, D., and Grob, L. M., "Variable Emissivity Through MEMS Technology," edited by G. B. Kromann, J. R. Culham, and K. Ramakrishna, *The Seventh Intersociety Conference on Thermal and Thermomechanical Phenomena in Electronic Systems*, IEEE, Piscataway, NJ, 2000 (Cat. No. 00CH37069), Vol. 2, pp. 264–270, Conference Paper (AN: 6754928).

[7] Karam, R. D., "Thermal Control Hardware," *Satellite Thermal Control for Systems Engineers*, edited by P. Zarchan, AIAA, Reston, VA, 1998, pp. 160–164.

[8] Mychkovsky, A., and Ponnappan, R., "Calorimetric Measurement of Emissivity in Space Conditions," AIAA 2005-961, Jan. 2005.

[9] Jaworske, D. A., and Skowronski, T. J., "Portable Infrared Reflectometer for Evaluating Emittance," *Proceedings of the Space Technology and Applications International Forum (STAIF-2000)*, edited by M. El-Genk, AIP Conference Proceedings, No. 504, American Institute of Physics Press, New York, 2000, pp. 791–796.

[10] Lasance, C. J. M., "The Thermal Conductivity of Air at Reduced Pressures and Length Scales," Electronics Cooling Online, Nov. 2002, http://www.electronics-cooling.com/html/2002_november_techdata.html [cited 22 Aug. 2006].

[11] Brewster, M. Q., *Thermal Radiative Transfer and Properties*, Wiley, New York, 1992, p. 89.